Available online at www.sciencedirect.com
ScienceDirect
Coastal Engineering 55 (2008) 423–430
Coastal Engineering
An International Journal for Coastal, Harbour and Offshore Engineers
www.elsevier.com/locate/coastaleng

Short communication

# Analysis of threshold and incipient conditions for sediment movement

A.A. Beheshti, B. Ataie-Ashtiani *

*Department of Civil Engineering, Sharif University of Technology, Tehran, Iran*

Received 7 June 2007; received in revised form 18 October 2007; accepted 3 January 2008
Available online 3 March 2008

**Abstract**

Prediction of threshold conditions and incipient motion is the essential issue for the study of sediment transport. This work compares existing empirical threshold curves proposed for Shields diagram, a method based on the concept of probability of sediment movement, and an empirical method based on movability number. These methods are used to predict the incipient motion conditions for experimental runs taken from various studies. Most of the experimental data, used in this work, have not been used before in derivation of alternative formulations for Shields diagram and other methods. The empirical threshold curves based on the Shields entrainment function was the least successful at predicting the measured incipient motion conditions, while the use of the movability number gives good predictions of critical shear velocity compared with experimental data.


*Keywords:* Sediment transport; Incipient motion; Shields diagram; Critical shear velocity; Movability number

## 1. Introduction

The concept of an entrainment threshold is the main issue of sediment transport in theory and practice. Sheilds (1936) has been the pioneer to describe the threshold shear stress at which the individual particles on a sedimentary bed, comprising nearly spherical shaped and uniform sediments, are on the verge of motion by a unidirectional stream flow. Shields diagram has extensively used for determination of incipient conditions for sediment movement problems. Dissatisfactions with this diagram have also been reported in the literature (e.g., Mantz, 1977; Yalin and Karahan, 1979; Smith and Cheung, 2004). The original Shields data showed considerable scatter and could be interpreted as representing a band rather than a well-defined curve (Buffington, 1999).

Due to the difficulty in defining the critical threshold conditions in the field, a number of empirical threshold curves have been developed (e.g., Chien and Wan, 1983; Hager and Oliveto, 2002; Cao et al., 2006). These empirical threshold curves represent relationships between the critical bottom shear stress and/or shear velocity and sediment characteristics, or between dimensionless parameters incorporating the principal flow and sediment properties. Marsh et al. (2004) compared some existing methods for predicting the incipient motion conditions of a uniform sand bed. It was shown that two of these methods, giving reasonable results, have difficulties with calculating of drag and lift coefficients.

The objectives of this study are to review and assess the most widely used threshold curves presented to original Sheilds (1936) curve, and exploring some of the major modifications to this curve. Also some of the alternative methods (Paphitis, 2001; Cheng and Chiew, 1999) are assessed. Finally, a method is presented and evaluated based on experimental datasets.

## 2. Empirical relationships for Shields type curves

Sheilds (1936) applied dimensional analysis and obtained a parameter which expresses a critical ratio of the applied bottom shear stress to the immersed weight of the grains (the Shields entrainment function, $\theta_{cr}=\tau_c / [(\rho_s-\rho)gd]$), and plotted it as a function of grain Reynolds number, $R_e{}^*=u_{*c}d/\nu$, where $\tau_c$ is the critical bottom shear stress, $\rho_s$ and $\rho$ are the sediment and fluid densities, $g$ is the acceleration due to gravity, $d$ is the particle

* Corresponding author. Fax: +98 21 66014828.
*E-mail address:* ataie@sharif.edu (B. Ataie-Ashtiani).

0378-3839/$ - see front matter © 2008 Elsevier B.V. All rights reserved.
doi:10.1016/j.coastaleng.2008.01.003

diameter, $u_c^*$ is the critical shear velocity, and $v$ is the kinematic viscosity of the fluid (at a particular water temperature).

Since the original publication of Sheilds (1936), the derived (threshold) curve has been extended and has received numerous revisions due to additional data having become available (Miller et al., 1977; Mantz, 1977; Yalin and Karahan, 1979; Buffington and Montgomery, 1997). A drawback of the Shields diagram is that the shear velocity appears on both axes. It has been argued by some investigators (Yalin, 1972; Yang, 1973) that the use of critical shear velocity $u_{*c}$ and bottom shear stress $\tau_c$ on both the abscissa and ordinate of the Shields curve (as dependent and independent variables, respectively) can present difficulties in interpretation, since they are interchangeable (through $u_c^* = \sqrt{\tau_c/\rho}$). Consequently, the critical bottom shear stress cannot be determined directly from the Shields curve but requires an iterative procedure.

In order to avoid trial and error solutions, alternative parameters are proposed by some researchers allowing direct computation of the critical shear velocity (or stress) through the entrainment function ($\theta_{cr}$) without recourse to an iterative procedure. The problem can be circumvented through the use of a dimensionless grain diameter defined as:

$$D_* = \left[(\rho_s - \rho)/\rho\left(g/v^2\right)\right]^{1/3} d \tag{1}$$

which is commonly used in threshold curves (Van Rijn, 1993). Liu (1957, 1958) developed a dimensionless grouping given by $u_*/w_s$, the movability number (as termed by Collins and Rigler, 1982) which has been used as an alternative to the Shields entrainment function. At this dimensionless number, $w_s$ is the settling velocity of particles.

Currently, many equations are available to account for Shields' inception curve. Bonnefille (1963) was one of the first to present the threshold in terms of $D_*$ and thus avoid the trial and error estimation of $u_{*c}$. Chien and Wan (1983) modified the Shields curve and presented a relationship between $\theta_{cr}$ and $D_*$ for six subdivided region. Hager and Oliveto (2002) subdivided the domain of interest into three portions, depending on $D_*$. At

Table 1
Existing formula and functions proposed for Shields type diagram

| Researchers | Formula |
|---|---|
| Bonnefille (1963) | $\theta_{cr} = \begin{cases} 0.118D_*^{-0.468} & D_* < 2.33 \\ 0.137D_*^{-0.648} & 2.33 \le D_* < 9.15 \\ 0.063D_*^{-0.298} & 9.15 \le D_* < 15.28 \\ 0.9D_*^{0.424} & 15.28 \le D_* < 58.3 \end{cases}$ |
| Chien and Wan (1983) | $\theta_{cr} = \begin{cases} 0.126D_*^{-0.44}, & D_* < 1.5 \\ 0.131D_*^{-0.55}, & 1.5 \le D_* < 10 \\ 0.0685D_*^{-0.27}, & 10 \le D_* < 20 \\ 0.0173D_*^{0.19}, & 20 \le D_* < 40 \\ 0.0115D_*^{0.30}, & 40 \le D_* < 150 \\ 0.052, & D_* \ge 150 \end{cases}$ |
| Paphitis (2001), mean curve | $\theta_{cr} = \frac{0.273}{1+1.2D_*} + 0.046\left(1 - 0.576e^{-0.02D_*}\right), \quad \left(0.01 < R_{e*} < 10^4\right)$ |
| Hager and Oliveto (2002) | $\theta_{cr} = \begin{cases} 0.120D_*^{-0.5} & D_* \le 10 \\ 0.026D_*^{0.167} & 10 < D_* < 150 \\ 0.06 & D_* \ge 150 \end{cases}$ |
| Cheng (2004) | $\theta_{cr} = 0.147D_*^{-0.29} \quad 0.114 \le D_* \le 35.4 \quad 0.02 \le R_{c*} \le 48.8$ |
| Sheppard and Renna (2005) | $\theta_{cr} = \begin{cases} 0.25 + 0.1D_*^{0.5}, & 0.1 < D_* < 3 \\ 0.0023D_* - 0.000378D_* \ln_e(D_*) + 0.23/D_* - 0.005, & 3 < D_* < 150 \\ 0.0575, & 150 < D_* \end{cases}$ |
| Cao et al. (2006) | $\theta_{cr} = \begin{cases} 0.1414R_d^{-0.2306}, & R_d < \approx 6.61 \\ \dfrac{\left[1 + (0.0223R_d)^{2.8358}\right]^{0.3542}}{3.0946R_d^{0.6769}}, & 6.61 \le R_d \le 282.84 \\ 0.045, & R_d > \approx 282.84 \end{cases}$ |
| | $R_d = d\sqrt{(S_s - 1)gd/v}, \quad S_s = \rho_s/\rho$ |

Florida Bridge Scour Manual (Sheppard and Renna, 2005) this domain also divided into three portions. Cao et al. (2006) developed an explicit formulation of the Shields diagram by deploying a logarithmic matching method. Paphitis (2001) presented a series of simple analytical formulae for the different threshold curves. He presented analytical formulae for lower (L) and upper (U) limits of the Shields diagram, on which $\theta_{cr}$ was plotted against $R_{e*}$. A single curve representing mean threshold values ($M$) was also presented. A similar analysis was performed with $D_*$ instead of $R_{e*}$. He also plotted the movability number ($u_* / w_s$) as a function of $R_{e*}$ and presented analytical formulae describing the single line curve and the limits of the envelopes. Cheng (2004) fitted a power function to data of incipient sediment motion in laminar flows, plotted as $R_{e*}$ versus $D_*$, with $R_{e*}$ varying from 0.02 to 48.8. All of these formula and functions that are assessed at this study are given in Table 1.

## 3. Data sources

The data included in the present study are from experiments that were undertaken in flumes with parallel side-walls under uniform steady flows. The associated sediments include a variety of natural and artificial grains, of quartz and near-quartz densities, and Coals, in beds consisting of nearly uniform sizes. The data compiled had their threshold conditions established either: a) through some form of visual definition; or b) from the extrapolation of transport rates to either zero or a low reference value. Table 2 summarizes all the sources utilized noting the material and fluid involved in the experiments. A total of 153 independent measurement data are considered.

## 4. Definitions of initiation of motion

In treating problems of initiation of motion, there is always a difficulty in defining what is meant by initiation of motion. In the following, some threshold definitions that used at data set considered above are briefly presented.

Table 2
Data sources, sedimentary material investigated and ambient fluid for experiments included in the analysis undertaken as part of the present investigation

| No. | Data source | Material/fluid |
|---|---|---|
| 1 | Rao and Sitaram (1999) | Sand/water |
| 2 | Sarmiento and Falcon (2006) | Sand/water |
| 3 | Dey and Raju (2002) | Gravel, coal/water |
| 4 | Dancey et al. (2002)[a] | Spherical glass bead/water |
| 5 | Mantz (1977) | Sand/water |
| 6 | White (1970) | Sand, crushed silica, lead glass spheres/water |
| 7 | Paintal (1971) | Gravel/water |
| 8 | Gilbert (1914) | Sand/water |
| 9 | Kramer (1935) | Sand/water |
| 10 | Casey (1935) | Sand/water |
| 11 | USWES (1935) | Sand/water |
| 12 | Sheilds (1936) | Sand, granite, fragments/water |
| 13 | Dey and Debnath (2000) | Sand/water |
| 14 | Kuhnle (1993) | Sand, gravel/water |

[a] Sediment packing density (ratio of total projected sediment area to bed area) varied from 2.6 to 91%.

Visual definitions of threshold are subject to the particular definition used by the individual investigator (Neill, 1968; Neill and Yalin, 1969). Kramer (1935) indicated four different bed shear conditions for sedimentary bed, namely, no transport, weak transport, medium transport, and general transport and he defined threshold shear stress to be that stress initiating general transport. White (1970) and Mantz (1977) made the visual observations of particle motion to define the terms first motion and incipient transport, respectively. White (1970) referred to the threshold of motion as the condition where a few grains move over a unit area. Through dimensional and similarity analysis Neill and Yalin (1969) obtained a dimensionless parameter threshold as $\varepsilon=(n / At)[\rho d^5 / (\rho_s-\rho)g]^{1/2}$ [Yalin (1972)], in which $n$ is the number of grain detachments occurring in a time $t$ over a given area of bed $A$. Yalin (1972) proposed setting the value of $\varepsilon$ to a small but nonzero value (on the order of $10^{-6}$) as the threshold condition.

Dancey et al. (2002) proposed a method for the characterization of the threshold condition for uniform sediment that accounts for 1) the availability of sediment; 2) the finite, nonzero, rate at which sediment is entrained; and 3) the inherent time scale of the physical process. A criterion was introduced where the level of bed activity at the threshold is set by a nonzero value of the probability of grain movement, $\Gamma$. The average number of grains that move in a time interval $t$ was given by $n=m\Gamma(t / \varsigma)$, in which $m$ = number of available sediment particles distributed over $A$, $\varsigma$ = average period between occurrences of the turbulent events, and $t/\varsigma$ represents the number of "events" in the time $t$. The threshold condition was obtained by assigning the value of $\Gamma=3.58\times10^{-5}$ as the threshold value.

Dey and Debnath (2000) defined the state at which a few sediment particles started to move as the threshold condition. In Dey and Raju (2002) experiments, the incipient condition was reached when all fractions of bed particles (on the surface) had movement over a period of time.

In contrast to visual definitions, the extrapolation methods are indirect; as such, the critical bottom shear stresses are estimated after extrapolation of the measured transport rates to either zero, or to a low reference value. Sheilds (1936) put forward a concept of sediment threshold that shear stress has a value for which the extrapolated sediment flux becomes zero. On the other hand, USWES (1935) set a concept of sediment threshold that tractive force brings about general motion of bed particles. For sediment particles less than 0.6 mm, this concept was found to be inadequate and general motion was redefined that sediment in motion should reasonably be represented by all sizes of bed particles and that sediment flux should exceed $4.1\times10^{-4}$ kg s/m. Thus, sediment threshold as a minimum flux was proposed. Paintal (1971) suggested from stochastic points of view that, due to the fluctuating nature of the instantaneous velocity, there is no mean shear stress below which there will be zero transport. With this consideration, the critical condition has to be defined as the shear stress that produces a certain minimal amount of transport. Yalin and Karahan (1979) showed that for steady laminar flows, uniform sediment begins

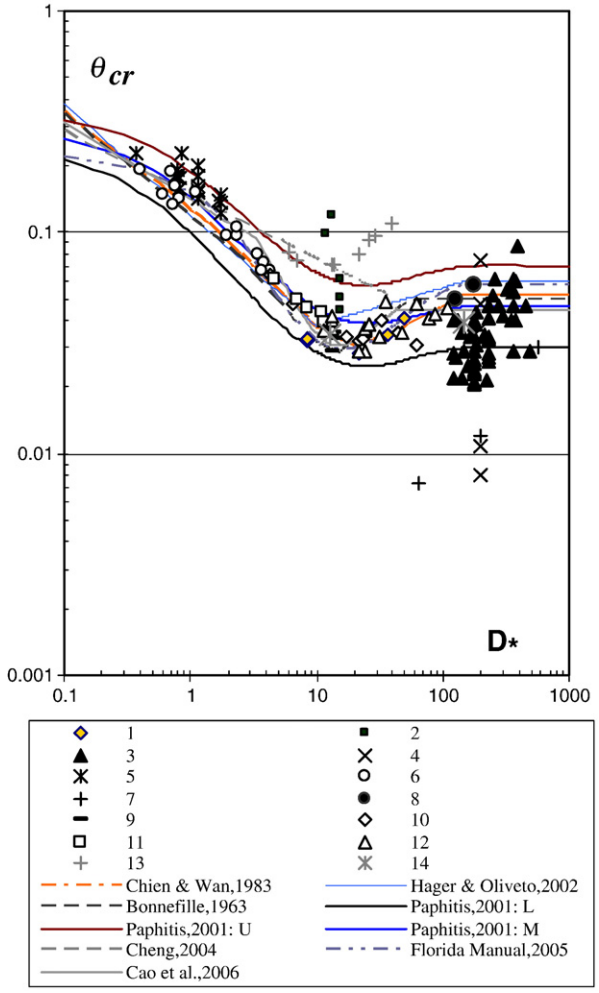


Fig. 1. Comparison of the curves ($\theta_{cr}$ versus $D_*$) proposed by different investigators with data reported in the various studies.

to move at a well-defined bed shear stress level and moves en masse. In an attempt to quantifiably relate the initiation of sediment motion to a small rate of transport, Parker et al. (1982) introduced a dimensionless bed load parameter $W=q^*/\tau$ (used successfully by other investigators, e.g. Kuhnle, 1993). $W$ is the transport rate at threshold (a value of $W=0.002$ was suggested as a reference transport rate corresponding to threshold conditions) and $q^*$ is the Einstein bed load parameter$=q/\left(\rho_s g\sqrt{(s-1)gd^3}\right)$, in which $q$ is the sediment transport rate in weight per unit width per second and $s$ = specific gravity of sand (see Einstein, 1942).

Following the approach of Sheilds (1936), Smith and Cheung (2004) determined the initiation of motion from measured pairs of shear stresses and transport rates at a range of flows that produce measurable transport. The $q^*=10^{-2}$ was interpreted as the onset of general motion. Observations made during the flume tests suggested the value of $q^*=10^{-4}$ for threshold condition.

Thus, a number of concepts of sediment threshold have been put forward. The numerous threshold definitions that are in use in the absence of a standardized definition of threshold lead to discrepancies in the data sets and introduce difficulties in making comparisons (Paintal,1971; Buffington and Montgomery, 1997).

## 5. Comparison of critical shear velocity prediction methods

Fig. 1 shows the comparison of the curves ($\theta_{cr}$ versus $D_*$) proposed by different investigators with data reported in the various studies for sediment threshold. The data symbols used in Fig. 1 can be identified by their symbol identification number listed in Table 2. The figure shows considerable disagreement with the proposed curves (Table 1). Dey and Raju (2002) and Dey and Debnath (2000) data are in complete disagreement with these curves. The experimental data showed considerable scatter and could be interpreted as representing a band rather than a well-defined curve. The discrepancy is primarily due to particle shape, random nature of the entrainment process, and the difficulty with defining criteria that adequately capture this feature, but other factors may also play a role. These comparisons show that the estimation for the initiation of motion in this way ($\theta_{cr}$ as a function of $D_*$) is not accurate to estimates for studying the transport of sediments. The ability of each of the above methods in predicting incipient motion are tested against experimental data and the correlation coefficients ($R^2$), slope of lines of best fit (slope), and root mean squared errors (RMSE) are given in Table 3. The correlation coefficients for Bonnefille (1963), Chien and Wan (1983), Paphitis (2001), Hager and Oliveto (2002), Florida Bridge Scour Manual (Sheppard and Renna, 2005), and Cao et al. (2006) proposed curves are similar, while for Cheng (2004) proposed curve it is lower. Paphitis (2001) method has a high $R^2$, a slope near unity, and a low RMSE. The RMSE is a measure of the deviation of the prediction from the line of perfect agreement (slope of 1). The low RMSE of Paphitis (2001) method shows that it predicts $u_{*c}$ values consistently close to the experimental values.

The use of the movability number ($u_*/w_s$) as a function of $R_{e*}$ was found to offer distinct advantages over the Shields entrainment Function ($\theta_{cr}$) as the inclusion of the settling velocity provides the implicit inclusion of any shape effects in the threshold determination (Collins and Rigler, 1982; Komar and Clemens, 1986).

The movability number is plotted as a function of the grain Reynolds number in Fig. 2. The single curve representing mean threshold values proposed by Paphitis (2001) is also presented

Table 3
Comparison of different methods for predicting incipient motion

| Formula | $R^2$ | RMSE | Slope |
|---|---|---|---|
| Bonnefille (1963) | 0.865 | 0.0122 | 1.153 |
| Chien and Wan (1983) | 0.861 | 0.0127 | 1.166 |
| Paphitis (2001) | 0.867 | 0.0109 | 1.079 |
| Hager and Oliveto (2002) | 0.867 | 0.0154 | 1.263 |
| Cheng (2004) | 0.7 | 0.0052 | 0.921 |
| Sheppard and Renna (2005) | 0.859 | 0.0146 | 1.238 |
| Cao et al. (2006) | 0.865 | 0.0106 | 1.0684 |

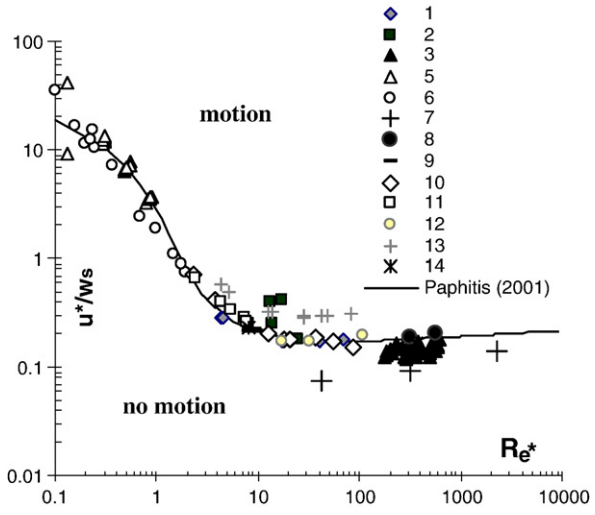


Fig. 2. The movability number as a function of the grain Reynolds number with the proposed formula by Paphitis (2001).

in Fig. 2. Paphitis (2001) presented a simple analytical formula for movability number as:

$$\frac{u_*}{w_s} = \frac{0.75}{R_{e*}} + 14e^{-2R_{e*}} + 0.01\ln R_{e*} + 0.115 \quad \left(0.1 < R_{e*} < 10^5\right). \tag{2}$$

The critical bottom shear stress cannot be determined directly from Paphitis (2001) formula (Eq. (2)), but requires an iterative procedure. Furthermore, the emergence of critical shear velocity $u_{*c}$ on both the abscissa and ordinate can present difficulties in interpretation.

To overcome these disadvantages, an alternative procedure is proposed in this study allowing direct computation of the critical shear velocity through the movability number without recourse to an iterative procedure. The movability number is plotted versus the dimensionless grain size in Fig 3. Simple functions are fitted to the existing data as:

$$\frac{u_{*c}}{w_s} = \begin{cases} 9.6674 \times D_*^{-1.57}, & D_* \le 10, \quad R^2 = 0.9954 \\ 0.4738 \times D_*^{-0.226}, & D_* > 10, \quad R^2 = 0.578 \end{cases}. \tag{3}$$

Since these equations are empirical, the break point at $D_*=10$ has no physical significance.

Figs. 2 and 3 display the significant improvement of the critical shear velocity prediction using the movability number compared to existing formulas based on the Shields entrainment Function. In Figs. 2 and 3, in order to meet the requirements of calculating the settling velocities, only experiments using sediment with a density near 2.65 kg/m$^3$ and water as the fluid are used. A total of 107 independent measurement sets were suitable, representing the ranges $R_{e*}=0.1$–$2304$, $d=0.015$–$22.2$ mm, and the bottom shear stress, $\tau=0.05$–$10.77$ kg/m/s$^2$. The settling velocities are calculated from the reported grain sizes and densities using an empirical relationship for natural particles.

Wu and Wang (2006) derived a general relation for settling velocity as

$$w_s = \frac{Av}{Bd'}\left[\sqrt{\frac{1}{4} + \left(\frac{4B}{3A^2}D_*'^3\right)^{1/a}} - \frac{1}{2}\right]^a \tag{4}$$

where $A$, $B$, and $a$ are coefficients and the sediment size is represented by the nominal diameter, $d'$. The tests against measurement data performed by Cheng (1997) have shown that for natural sediment the values of 32–34 for $A$ give better predictions than the value of 24 that correspond to the Stokes' law for spherical particles. Wu and Wang (2006) calibrated the coefficients $A$, $B$, and $a$ by using extensive data collected from different countries and regions, as

$$A = 53.5e^{-0.65S_f}; \quad B = 5.65e^{-2.5S_f}; \quad a = 0.7 + 0.9S_f \tag{5}$$

where $S_f$ is the Corey shape factor. Eq. (4) is applied with the coefficients $A$, $B$, and $a$ determined by Eq. (5). It is an explicit relation of the settling velocity for given sediment size and shape factor so that it can be easily used. The Corey shape factor of the sediment used in this study is assumed to be 0.7, which is usually taken as the most common value for naturally shaped sediments (Interagency Committee 1957; Dietrich 1982; Cheng 1997; Camenen, 2007). For this value of shape factor, Eq. (5) corresponds to $A=33.9$, $B=0.98$, and $a=1.33$. Also, the sediment size in collected data at this study is characterized by the sieve diameter, which is approximately converted to the nominal diameter by dividing by a factor of 0.9 (Raudkivi, 1990).

Fig. 4 shows the comparisons between experimental data and proposed formulas at this study, Eq. (3), Paphitis (2001) ($u_*/w_s$ versus $R_{e*}$), Eq. (2), Paphitis (2001) ($\theta_{cr}$ versus $D_*$), Table 1, and the Cheng and Chiew (1999) method. Cheng and Chiew (1999) performed a theoretical analysis of the initiation of

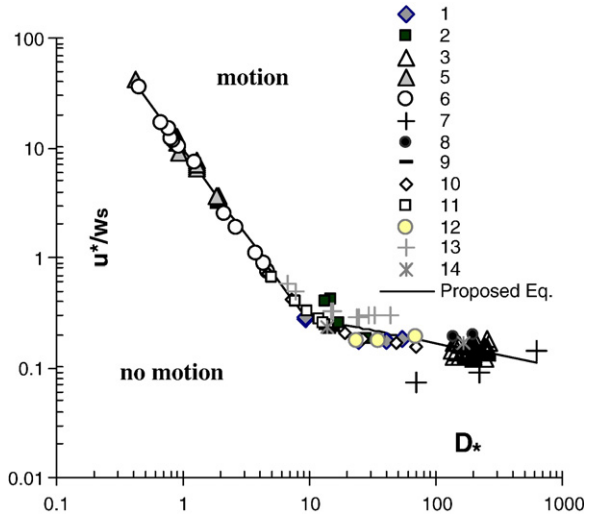


Fig. 3. The movability number as a function of the dimensionless grain diameter with the proposed regression lines.

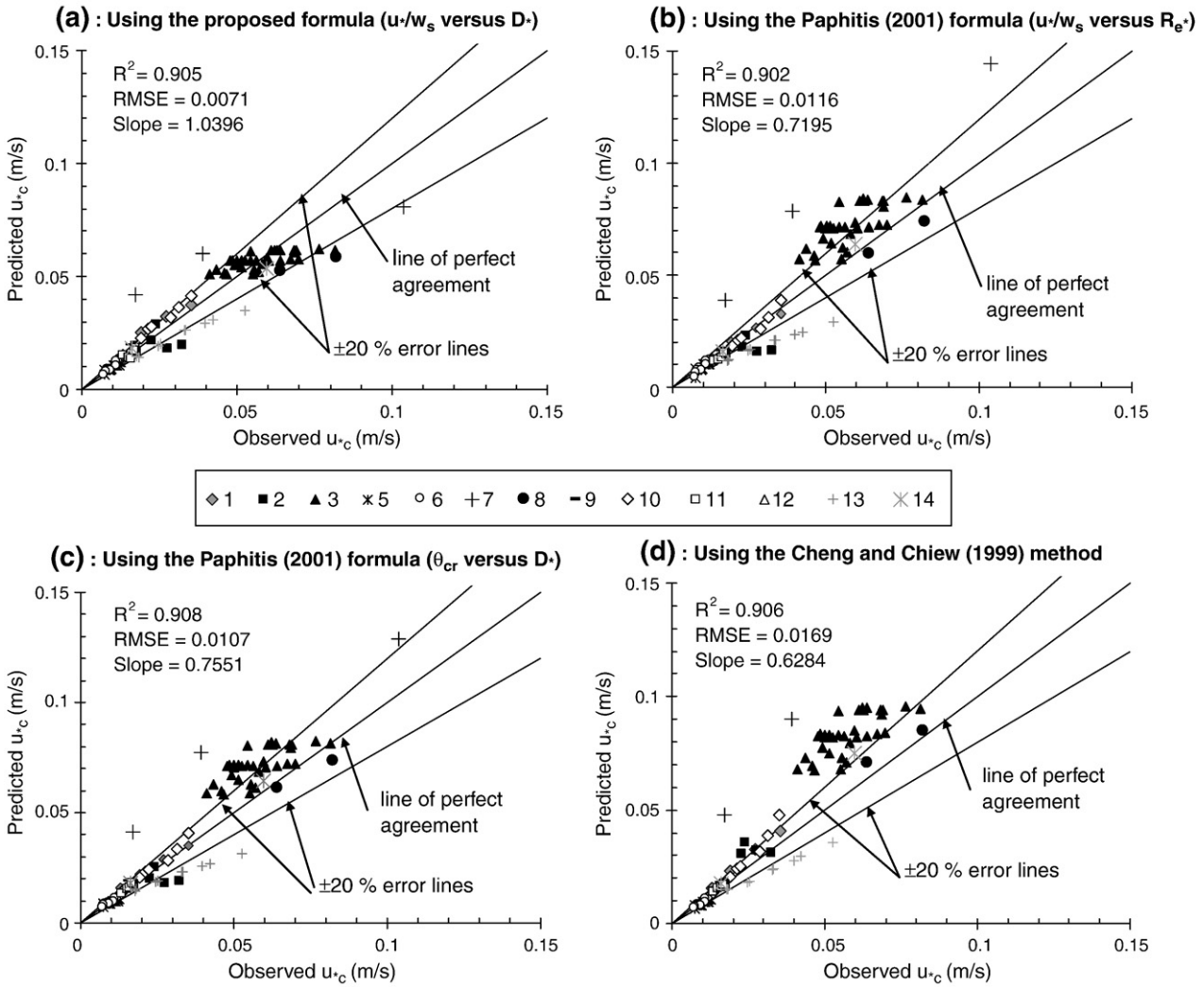


Fig. 4. Comparison of experimentally derived and predicted critical shear velocity: (a) proposed method, (b) Paphitis (2001) method based on movability number, (c) Paphitis (2001) method based on the Shields entrainment Function ($\theta_{cr}$), and (d) the Cheng and Chiew (1999) method.

sediment suspension based on the concept of probability of suspension. The probability of initiation of sediment suspension from bed was presented as:

$$P = 0.5 - 0.5\sqrt{1 - \exp\left(-\frac{2}{\pi}\frac{w_s^2}{\sigma^2}\right)} \tag{6}$$

where $w_s$ can be computed using Eq. (4) for natural sediment particles and $\sigma$ is the RMS value of the vertical velocity fluctuations and can be evaluated as:

$$\frac{\sigma}{u_*} = 1 - \exp\left[-0.025\left(\frac{u_* y}{\nu}\right)^{1.3}\right] \tag{7}$$

where $y$ = distance from the bed ($y$=2.75$d$). When the probability of suspension approached an infinitesimal value of $10^{-7}$, the computed relationship of the Shields parameter and the particle Reynolds number using Eqs.(6) and (7) approximated very well to the updated Shields diagram for the incipient sediment motion.

As can be shown from Fig. 4, the correlation coefficients for all methods are similar. The proposed method at this study has a high $R^2$, a slope of line of best fit (slope) near unity, and a low root mean squared error, RMSE. The RMSE and slope of line of best fit for Paphitis (2001) formulas based on the movability number, Fig. (4-b), and Shields entrainment function, Fig. (4-c), are similar. The Cheng and Chiew (1999) method has a slightly lower slope and higher RMSE compared to other methods, indicating a slightly poorer prediction of experimental values, Fig. (4-d). The low RMSE of the proposed method shows that it predicts $u_{*c}$ values consistently close to the experimental values. Furthermore, the slope for this method is closer to unity than other methods, indicating that it may be a more robust method across a wider range of prediction scenarios. For proposed method, most of the data points lay within the ±20% error lines, Fig. (4-a).

## 6. Conclusions

This paper compared most widely used threshold curves presented to Shields diagram, a method based on the concept of probability of sediment movement, and empirical methods based on movability number ($u_* / w_s$) for predicting incipient motion. The primary aim of the present investigation was to re-examining the relationship between the parameters employed in some of the most widely used threshold diagrams. Towards this objective, an extensive set of existing experimental data set on sediment threshold under unidirectional flow conditions was used. By utilizing these data, it was found that the empirical threshold curves based on the Shields entrainment function was the least successful at predicting the measured incipient motion conditions. Of these proposed curves it may be argued that the Paphitis (2001) single curve is useful for prediction of critical shear velocity ($u_{*c}$) because it has both a high $R^2$ (=0.87), a slope near unity, and a low RMSE (=0.0109) compared to other empirical curves.

The use of the movability number was found to be more adequate in the threshold determination. The proposed formula at this study based on the movability number (as a function of dimensionless grain size) has high $R^2$ (=0.91) and low RMSE (0.0071) compared to other methods. For this method, most of the data points lay within the ±20% error lines. Paphitis (2001) methods based on the movability number and Shields entrainment function provided a similar level of capacity to predict experimental observations. The Cheng and Chiew (1999) Method has a slightly poorer prediction of experimental values. Of these four methods it may be argued that the proposed method is useful to use because it is computationally simpler, allowing direct computation of the critical shear velocity.

## References


Bonnefille, R., 1963. Essais de synthese des lois de debut d'entrainment des sediment sous l'action d'un courant en regime uniform. Bull. Du CREC, No. 5, Chatou.

Buffington, J.M., 1999. The legend of A. F. Shields. J. Hydraul. Eng. 125 (4), 376–387.

Buffington, J., Montgomery, D., 1997. A systematic analysis of eight decades of incipient motion studies, with special reference to gravel bed rivers. Water Resour. Res. 33 (8), 1993–2029.

Camenen, B., 2007. Simple and general formula for the settling velocity of particles. J. Hydraul. Eng. 133 (2), 229–233.

Cao, Z., Pender, G., Meng, J., 2006. Explicit formulation of the Shields diagram for incipient motion of sediment. J. Hydraul. Eng. 132 (10), 1097–1099.

Casey, H., 1935. Uber geschiebebewegung. Mitt. Preuss. Versuchsanst, Wasserbau Schiffbau 19, 86 pp.

Cheng, N.S., 1997. Simplified settling velocity formula for sediment particle. J. Hydraul. Eng. 123 (2), 149–152.

Cheng, N.S., 2004. Analysis of bedload transport in laminar flows. Adv. Water Resour. 27, 937–942.

Cheng, N.S., Chiew, Y.M., 1999. Analysis of initiation of sediment suspension from bed load. J. Hydraul. Eng. 125 (8), 855–861.

Chien, N., Wan, Z.H., 1983. Mechanics of Sediment Movement. Science Publications, Beijing. (in Chinese).

Collins, M.B., Rigler, J.K., 1982. The use of settling velocity in defining the initiation of motion of heavy mineral grains, under unidirectional flow. Sedimentology 29, 419–426.

Dancey, C.L., Diplas, P., Papanicolaou, A., Bala, M., 2002. Probability of individual grain movement and threshold condition. J. Hydraul. Eng. 128 (12), 1069–1075.

Dey, S., Debnath, K., 2000. Influence of streamwise bed slope on sediment threshold under stream flow. J. Hydraul. Eng. 126 (4), 255–263.

Dey, S., Raju, U.V., 2002. Incipient Motion of Gravel and Coal Beds. Sadhana 27 (Part 5), 559–568 Part 5 (Printed in India).

Dietrich, W.E., 1982. Settling velocity of natural particles. Water Resour. Res. 18 (6), 1615–1626.

Einstein, H.A., 1942. Formulas for the transportation of bed-load. Trans. ASCE 107, 561–597.

Gilbert, G.K., 1914. The transportation of debris by running water. U.S. Geol. Surv. Prof. Pap., 86. 263 pp.

Hager, W.H., Oliveto, G., 2002. Shields' entrainment criterion in bridge hydraulics. J. Hydraul. Eng. 128 (5), 538–542.

Interagency Committee, 1957. Some fundamentals of particle size analysis: a study of methods used in measurement and analysis of sediment loads in streams. Rep. No. 12, Subcommittee on Sedimentation, Interagency Committee on Water Resources. St. Anthony Falls Hydraulic Laboratory, Minneapolis.

Komar, P.D., Clemens, K.E., 1986. The relationship between a grain's settling velocity and threshold of motion under unidirectional currents. J. Sediment. Petrol. 56 (2), 258–266.

Kramer, H., 1935. Sand mixtures and sand movement in fluvial models. Trans. ASCE 100, 798–878.

Kuhnle, R., 1993. 'Incipient motion of sand–gravel sediment mixtures. J. Hydraul. Eng. 119 (12), 1400–1415.

Liu, H.K., 1957. Mechanics of sediment ripple formation. J. Hydraul. Div. 83 (2), 1–23.

Liu, H.K., 1958. Closure: mechanics of sediment ripple formation. J. Hydraul. Div. 84 (5), 5–31.

Mantz, P., 1977. Incipient transport of fine grains and flakes by fluids—extended Shields diagram. J. Hydraul. Div. 103 (6), 601–615.

Marsh, N.A., Western, A.W., Grayson, R.B., 2004. Comparison of methods for predicting incipient motion for sand beds. J. Hydraul. Eng. 130 (7), 616–621.

Miller, M.C., McCace, I.N., Komar, P.D., 1977. Threshold of sediment motion under unidirectional currents. Sedimentology 24, 507–527.

Neill, C.R., 1968. A re-examination of the beginning of movement for coarse granular bed material. Unpublished Technical Report, 68. Hydraulic Research Station.

Neill, C.R., Yalin, M.S., 1969. Quantitative definition of beginning of bed movement. J. Hydraul. Div. 95 (1), 585–588.

Paintal, A., 1971. Concept of critical shear stress in loose boundary open channels. J. Hydraul. Res. 9 (1), 91–113.

Paphitis, D., 2001. Sediment movement under unidirectional flows: an assessment of empirical threshold curves Coas. Eng. 43, 227–245.

Parker, G., Klingeman, P.C., McLean, D.G., 1982. Bedload and size distribution in paved gravel-bed streams. J. Hydraul. Div. 108, 544–571.

Rao, A.R., Sitaram, N., 1999. Stability and mobility of sand-bed channels affected by seepage. J. Irrig. Drain. Eng. 125 (16), 370–379.

Raudkivi, A.J., 1990. Loose Boundary Hydraulics, 3rd ed. Pergamon, Tarrytown, N.Y.

Sarmiento, O.A., Falcon, M.A., 2006. Critical bed shear stress for unisize sediment. J. Hydraul. Eng. 132 (2), 172–179.

Sheppard, D. Max, Renna, Rick, 2005. Florida Bridge Scour Manual. Florida Department of Transportation, 605 Suwannee Street, Tallahassee, FL 32399-0450.

Sheilds, A., 1936. Anwendung der Ahnlichkeitsmechanik und Turbulenz-forschung auf Geschiebebewegung. Mitteilungen der Preuss. Versuchsanst. f. Wasserbau u. Schiffbau, Heft 26, Berlin.

Smith, D.A., Cheung, K.F., 2004. Initiation of motion of calcareous sand. J. Hydraul. Eng. 130 (5), 467–472.

U.S. Waterways Experimental Station, USWES, 1935. Study of river-bed material and their use with special reference to the Lower Mississippi River. Vicksburg MS, Paper, 17.

Van Rijn, L.C., 1993. Principles of Sediment Transport in Rivers, Estuaries and Coastal Seas. Amsterdam, Aqua Publications.

White, S., 1970. Plane bed thresholds of fine grained sediments. Nature (London) 228, 152–153.

Wu, W., Wang, S.S.Y., 2006. Formulas for sediment porosity and settling velocity. J. Hydraul. Eng. 132 (8), 858–862.

Yalin, M.S., 1972. Mechanics of Sediment Transport. New York, Pergamon.

Yalin, M.S., Karahan, E., 1979. Inception of sediment transport. J. Hydraul. Div. 105 (11), 1433–1443.

Yang, C., 1973. Incipient motion and sediment transport. J. Hydraul. Div. 99 (10), 1679–1704.